Experimental and modelling study of phenol combustion and oxidation

Nicolas Delort, Ismahane Meziane, Olivier Herbinet, Hans-Heinrich Carstensen, Frédérique Battin-Leclerc

Experimental and modelling study of phenol combustion and oxidation

Nicolas Delort[a], Ismahane Meziane[a], Olivier Herbinet[a], Hans-Heinrich Carstensen[b], Frédérique Battin-Leclerc [a,*]

[a]Université de Lorraine, CNRS, LRGP, F-54000 Nancy, France
[b]Fundación Agencia Aragonesa para la Investigación y el Desarrollo (ARAID), Zaragoza, Spain

---

Abstract

Despite of its central importance in the chemistry of aromatic compounds and fuels derived from biomass, only few experimental studies about on phenol combustion can be found in literature. In this paper, unique measurements of the adiabatic laminar burning velocities of phenol are presented, together with the first experimental study of the oxidation of this molecule in a jet-stirred reactor. The burning velocities were measured with a flat-flame burner using the heat-flux method for a fresh gas temperature of 398 K and equivalence ratios from 0.7 to 1.35. In the reactor experiments, the oxidation of a stoichiometric mixture of phenol highly diluted in helium was investigated at temperatures between 600 and 1100 K at near-atmospheric pressure. The mole fraction of the reactants, as well as 32 products, mainly carbon monoxide, carbon dioxide, methane, acetylene ethylene, acrolein, cyclopentadiene, benzene, naphthalene and dibenzofuran, were recorded.

Based on previous literature work, a new detailed kinetic model is developed based on several published sub-mechanisms and updated considering rate constants taken from recent literature studies or calculated at the CBS-QB3 or G4 level of theory. This model leads to a significantly improved prediction of the phenol burning velocities compared to literature models, as well as a reasonable prediction of most species mole fractions during phenol oxidation in the jet-stirred reactor. Sensitivity analyses as well as flow rate analyses are discussed to explain the obtained model improvements.

Keywords: Phenol; Laminar burning velocity; Jet-stirred reactor; Detailed kinetic model.

---

*Corresponding author.

Information for Colloquium Chairs and Cochairs, Editors, and Reviewers

Note: The explanatory material in italic font on this page should be removed prior to manuscript submission.

1) Novelty and Significance Statement

The novelty of this research consists in the first measurements of the laminar burning velocity of phenol, a solid fuel and the smallest oxygenated molecule including a phenyl ring, which is of central importance in the chemistry of aromatic compounds. It also reports the first experimental study of phenol oxidation in a jet-stirred reactor including the quantification of 32 products and the development of a new model able to satisfactorily reproduce this new data, better than existing literature models.

2) Author Contributions

- ND: Performed LBV measurements, Developed the kinetic model, Performed kinetic analyses, Wrote the paper;
- IM: Performed JSR measurements, Analyzed data, Reviewed the paper;
- OH: Supervision, Set-up experiments, Analyzed data, Reviewed the paper;
- HHC: Performed theoretical calculations, Reviewed the paper;
- FBL: Supervision, Analyzed data, Wrote the paper.

3) Authors' Preference and Justification for Mode of Presentation at the Symposium

The authors prefer **OPP** presentation at the Symposium, for the following reasons:

- Work on a reactant of pivotal importance in the combustion chemistry of aromatic compounds, thus of wide interest.
- Unique measurements of the laminar burning velocity of phenol.
- First experimental study of phenol oxidation in a jet-stirred reactor, including the quantification of 32 products.
- Rate constant revision based on literature and theoretical calculations with wide discussion possibilities,
- Development of a new model leading to significantly improved predictions compared to literature ones.

1. Introduction

Phenol is a species of central importance in all detailed kinetic mechanisms proposed to model the oxidation of monoaromatic compounds [1,2] as it is a key intermediate both involved in the PAH formation and in the formation of smaller species. Indeed, the CO elimination reactions either directly from phenol, or through its resonance-stabilized phenoxy radical, are prominent ring contractions that convert an aromatic six-membered ring species into a five-membered ring product.

Phenol is the smallest aromatic molecule found in notable amounts in bio-oils obtained by the fast pyrolysis of biomass [3,4]. It is also produced during the catalytic lignin solvolysis, a promising process to transform lignin, usually a waste of bioethanol production, into valuable biofuels [5]**Erreur ! Source du renvoi introuvable.**. This process is the target of the EHLCATHOL European project (https://ehlcathol.eu/).

Despite its above-mentioned importance, there is only a very limited number of experimental studies available on phenol pyrolysis and combustion, certainly due to the fact that it is solid at room temperature. Two of them were performed using shock-tubes by He et al. [6] and Horn et al. [7] allowing to derive rate constants of, respectively, the H abstractions by H-atoms and OH radicals and the CO-elimination from phenol. Three flow reactors studies are known [8–10], among which two focused on pyrolysis [8,10], while the work by Brezinsky et al. [9] in 1998 investigated phenol oxidation around 1170 K, at atmospheric pressure over a range of equivalence ratios, 0.64-1.73. A total of 9 products were quantified by gas chromatography, namely, methane, carbon monoxide, acetylene, carbon dioxide, C_3 unsaturated hydrocarbons, cyclopentadiene, 1,3-butadiene, benzene, and naphthalene.

Since the work of Alzueta et al. [1] in 2000 on benzene followed by the study of Bounaceur et al. [11] on toluene, phenol is a key species found in all the detailed kinetic models dealing with the oxidation of aromatic compounds, e.g. [4,12–14]. In 2020, Pratali Maffei et al. [15] revisited the rate constants of the main reactions for phenol pyrolysis based on theoretical calculations. These new values were used in the CRECK model to satisfactorily simulate the experimental data available for phenol pyrolysis [7,9,10].

To our best knowledge, phenol oxidation has not been studied in a reactor since the work by Brezinsky et al. [9]. Furthermore, no experimental flame data for phenol is available in literature. The first purpose of the current paper is therefore to present the first measurements of laminar burning velocities (LBV) for phenol, as well as the first product quantifications during its oxidation in a jet-stirred reactor. Its second objective is to update an existing detailed kinetic model for aromatic compounds [2,16] using recent theoretical calculations in order to improve the predictions of the newly obtained experimental data.

2. Experimental methods and results

This section starts by describing the setups used in LRGP-Nancy to measure LBVs with a laminar flat flame burner and to quantify products during fuel oxidation in a heated JSR. A special focus will be on adaptions made to handle phenol, a solid reactant at room temperature ($T_{melting}$ = 314 K), and with low volatility ($T_{boiling}$ = 455 K) [5]. It is followed by a description on the obtained experimental results.

2.1 Experimental methods

The methods used in flame and in JSR, as well as needed adaptations are described below:

2.1.1. Flame measurements

The measurements of LBV were performed under atmospheric pressure based on the heat-flux method [17] using a flat flame burner, a set-up already utilized for measuring LBV of a wide range of organic reactants, among which are anisole and guaiacol [16]. The adiabaticity of the flame is indicated by the flat shape of the temperature profile across the burner plate verified by eight thermocouples. At these conditions, the velocity of the flame is equal to the velocity of the gases.

2.1.2. JSR measurements

The JSR consists of a 92 cm^3 fused silica sphere including four injection nozzles located at the center of the sphere to provide turbulent jets for an efficient mixing. Details can be found in previous publications, e.g. including the recent ones reporting on arenes [2] and guaiacol oxidation [16]. The gas mixture leaving the JSR, maintained at a pressure of 1.067 bar (residence time 2s), was analyzed by three gas chromatographs (GCs). The first GC is used for the quantification of oxygen. It was equipped with a Carbosphere packed column and a thermal conductivity detector. The second GC was fitted with a Q-Bond capillary column and a flame ionization detector (FID), preceded by a methanizer. It served for the quantification of CO, CO_2 and organic compounds containing from two carbon atoms, such as acetylene or ethylene, up to compounds with 6 carbon atoms, such as benzene. A third GC, which was equipped with a HP-5 capillary column and both a mass-spectrometer and a FID detector, was used for the quantification of the heaviest compounds (C_{6+}). The identification of reaction products was performed using a GC equipped with both types of capillary columns and coupled to a mass spectrometer and an FID (CG-MS-FID).

2.1.3. Phenol specific adaptations

In both set-ups, the flow rates of oxygen and carrier gas (N_2 for LBV, He in JSR) are regulated by mass flow controllers. The liquid fuel flow rate is monitored using a Cori-Flow mass flow controller, which is fed by a pressurized stainless-steel fuel tank and connected to an evaporation chamber also alimented by the carrier gas. After mixing with oxygen, the gaseous mixture is transferred by a heated line (T = 398 K) to the plenum chamber preceding the burner or to the preheating zone of the JSR. The relative uncertainty of the flow rates is ±0.5%. Phenol was provided by Merck with a purity above 99%; oxygen (purity ≥ 99.999%), helium (purity ≥ 99.999%), and nitrogen (purity: 99.995%) were provided by Messer France.

The use of solid phenol required the following main modifications to the feeding system. The fuel container was kept in a hot water bath until it was used to fill the fuel tank. The tank and all the lines transferring liquid to the evaporator were wrapped by electric heating to ensure a constant temperature of 353 K, i.e. above phenol melting point.

The second modification concerns the analyses of the reacted gases. At the outlet of the JSR, instead of analyzing the heavy molecules (>C_6) after on-line transfer to the GC as in [2], those were cryogenically trapped. The content of the trap was then dissolved in acetone and injected with an auto-sampler into the GC-MS-FID.

2.2 Experimental results

All the obtained experimental data are provided in in an Excel spreadsheet in Supplementary Materials (SM). In all figures of this section, symbols represent experimental results and lines simulations using COLIBRI v3 model (see next section).

2.2.1. Flame results

The LBV measurements are displayed in Figure 1. The range of equivalence ratios (Φ), from 0.7 to 1.35, is limited by flame stability. For these ratios, the flame shape was flat in lean mixtures and there was neither liquid condensation at the walls nor cellular instabilities in rich mixtures. The uncertainties indicated in Figure 1 are calculated for each individual experiment and take into account the uncertainties of devices: those of the flow controllers, of the used K-type thermocouples in the plate and of the T-type thermocouple monitoring the chamber temperature, as well as minor sources of uncertainties such as distortion and edge effects. The small variations of the chamber temperature and the adiabatic condition consideration both lead to uncertainties attributed to the user; they are also considered. More details about the experimental uncertainties are given in SM.

The obtained LBV profile shows a maximum burning velocity (LBV_{max}) of 59.2 cm/s at around Φ = 1.1, and a slightly steeper decline towards higher Φ than towards lower Φ. The data show that the burning velocity of phenol is slightly higher than that of toluene (LBV_{max} = 56.0 cm/s [18], measured with the same setup under the same conditions) and almost equal to that of anisole (LBV_{max} = 60.0 cm/s [16]).

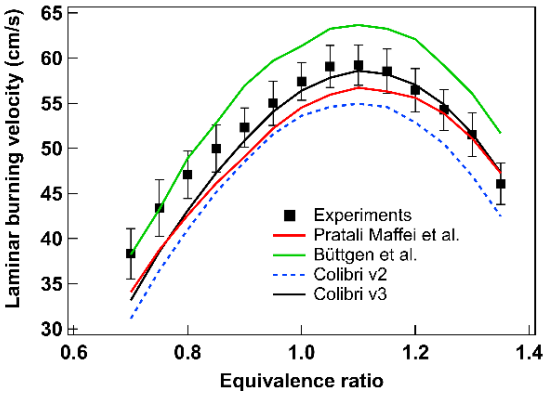

Fig. 1. Phenol LBV for fresh gases at 398 K. Simulations using literature models (Colibri v2 [16], Büttgen et al. [14], Pratali Maffei et al. [15]) are added.

2.2.2. JSR results

The mole fractions of both reactants at the outlet of the JSR are presented in Figure 2. The uncertainty of the O_2 mole fraction is around ±5%, in contrast to that of phenol, which is ±10%. Figure 2 indicates that phenol consumption starts at the chosen conditions around 900 K and complete consumption is reached above 1050 K. A similar reactivity profile is observed for oxygen; however, it is not yet completely

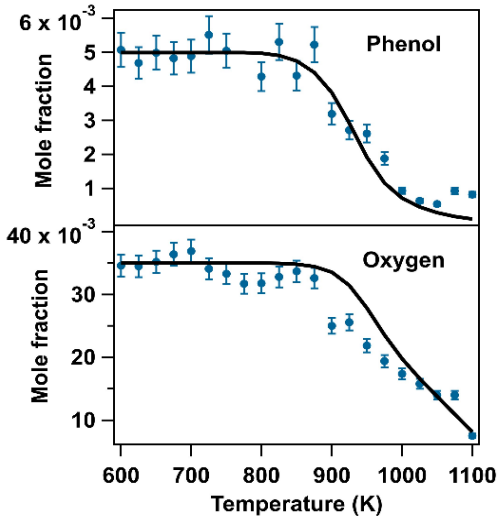

Fig. 2. JSR mole fractions of phenol and O_2.

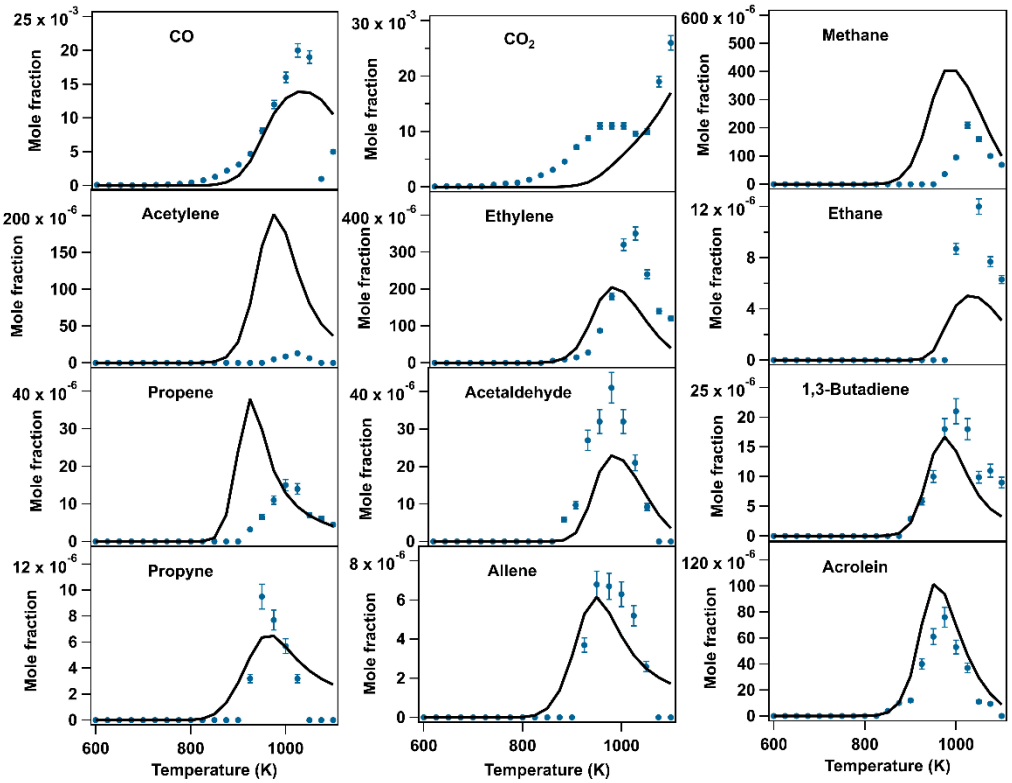

Fig.3. Mole fraction profiles of C_1-C_4 products quantified during the JSR oxidation of phenol.

consumed even at the highest temperatures. One possible reason for this – oscillations – is discussed later.

In this study, 32 products were identified and quantified and, in addition, traces of 2-butene, cumene and phenyloxirane, were detected.

The quantified products can be grouped into four categories: (1) Five C_1-C_4 oxygenated species: CO, CO_2, acetaldehyde (CH_3CHO), acrolein (CH_2CHCHO), and furan, (2) 13 C_1-C_5 hydrocarbons: methane (CH_4), acetylene (C_2H_2), ethylene (C_2H_4), ethane (C_2H_6), propene (C_3H_6), allene (a-C_3H_4), propyne (p-C_3H_4), 1-butene (1-C_4H_8), 1,3-butadiene (1,3-C_4H_6), 1,2-butadiene (1,2-C_4H_6), 2-butene (2-C_4H_8), 1,3-cyclopentadiene, cyclopentene, and 1,3-cyclohexadiene, (3) 6 aromatic hydrocarbons: benzene, toluene, styrene, ethylbenzene, indene, 3-methyl-1H-indene, and naphthalene, (4) 8 oxygenated aromatics: benzaldehyde, o-cresol, methylbenzaldehyde, 1-indanone, dibenzofuran, a $C_{12}H_8O_2$ species, 2,5'-biphenyldiol and 2,2':5',2"-diepoxy-p-terphenyl. The formulas, and the possible names and structures of the cyclic compounds are given in Table S1 in SM. The $C_{12}H_8O_2$ might most probably be 2-phenoxyphenol, but the formation of 3-hydroxydibenzofuran and dibenzo-1,4-dioxin cannot be discarded.

Concerning the $C_{12}H_{10}O_2$ species, we assume that they were formed through phenoxy radical recombination. 2,5'-biphenyldiol provided the best match with the mass spectrum of the NIST08 library. The relative stability of possible structures will be discussed in the text.

Calibrations were performed by injecting standards for C_1-C_2 species, with a maximum relative error in mole fractions around ±5%. Otherwise, the effective carbon number method was used with an uncertainty of 10%, possibly higher for products analyzed off-line, e.g., 20 % for C_{12}-C_{18} species.

Figures 3 and 4 present the experimental mole fractions of the most significant products quantified during the JSR oxidation of phenol; more products are shown in Figure S2 in SM.

The two products found in the largest amounts are CO and CO_2. However, as already noticed in [2,16], the mole fractions of CO_2 is overestimated, likely because of an artifact during the sampling or the analysis, partly explaining the large positive deviations around +30% in the carbon balance displayed in Table S2 in SM. As in [2], this does not affect the formation of the other products.

Another factor explaining the observed deviation in the carbon balance is the phenomenon of oscillations (a transient evolution of species mole fractions with time), also reported in our previous work [2,16],

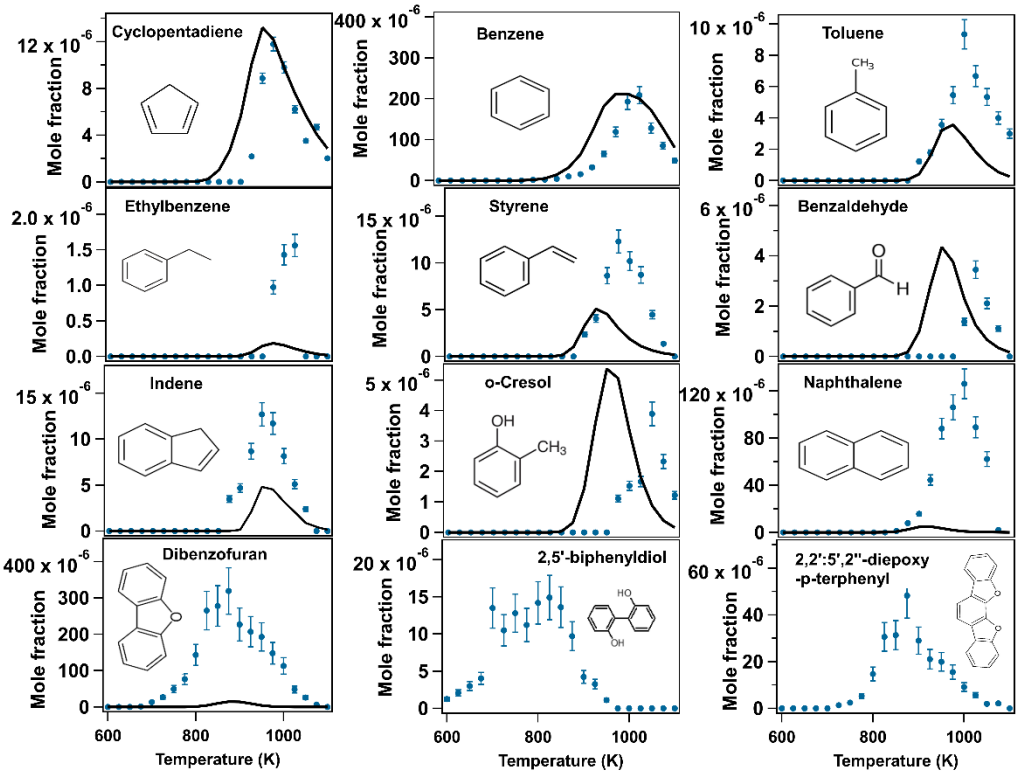

Fig.4. Mole fraction profiles of the main C_5-C_{12} products quantified during the JSR oxidation of phenol.

which occurs from 1050 K and explains the strange evolution of phenol and CO mole fractions at and above this temperature.

Besides CO and CO_2, other products found in significant concentrations, e.g., with a maximum mole fraction above 100 ppm, are methane, dibenzofuran, ethylene, benzene, and naphthalene. While notable phenol consumption is observed from 900 K, some products with non-negligible yields are already detected starting at 700 K. As it is shown by the selectivity analysis displayed in Figure S1 in SM, the aromatic compounds with the largest selectivity at 700 K are 4-hydroxydibenzofuran and dibenzofuran. Except for CO, naphthalene has the largest selectivity at 900 K at the start of phenol conversion.

3. Detailed kinetic modeling

Figures 1 and S3-S5 show a comparison between the present experimental LBV and JSR mole fractions and simulation using literature models considering phenol: COLIBRI v2 [16], the model of Büttgen et al. [14], that of Yuan et al. for anisole [19], and that of Pratali Maffei et al. [15]. All the simulations displayed in the paper and its SM were performed using CHEMKIN-Pro software [20] with GRAD and CURV parameters equal to 0.1 for LBV calculations. While most JSR mole fraction are reasonably well predicted by literature models, especially by COLIBRI v2 [16], this is not the case for the LBV data for which significant deviations are observed. More specifically, simulations using COLIBRI v2 and Pratali Maffei et al. [15] model underestimate the measured maximum LBV by about 4 cm/s and 3 cm/s respectively. In contrast, the model of Büttgen et al. [14] overestimates the maximum experimental LBV by 5 cm/s. Numerical convergence with a refined grid has not been successfully reached with Yuan et al. model [19], which presents a high stiffness. The deviations of LBV predictions between different models is mainly due to the C_5H_XO submechanism, notably composed of reaction of cyclopentadienone, cyclopentadienol and their derived radicals. As shown by the sensitivity analysis in Fig. 5e, these reactions have a strong influence on the LBV. Many reactions of the COLIBRI model are lacking in the Büttgen and the CRECK ones. Additionally, some species are not considered in the CRECK model. The rate constants of inhibiting reactions are also far lower in Büttgen model compared to those of COLIBRI. Notably, Fig. S20 in Supplementary Material compares the termination reaction of cyclopentadienyl-ol radicals with H-atoms yielding cyclopentadienol found in COLIBRI and in the model of Büttgen. The rate constant of Büttgen model is two and one orders of magnitude lower at 1000 K and 1400 K, respectively. The inhibiting effect of the C_5H_XO submechanism is globally less present in the Büttgen model.

The unsatisfactory LBV simulation results call for an updated and extended kinetic model. Such a model, named COLIBRI v3, is developed in this study. It contains 477 species and 3007 reactions and is provided in SM along with its thermochemical data and transport data.

3.1. Development of a new model

The COLIBRI v3 model is an offspring of the COLIBRI v2 model, which allows a satisfactory simulation of the combustion of guaiacol, anisole, xylene isomers and toluene [2,16]. In addition to few in-house reactions added in order to explain the formation of minor products, this previous model is mainly built as a merge of 6 literature models in order to combine their accuracy, but keeping good convergence performances: (1) the Galway reaction base [21], (2) the toluene model of Yuan et al. [12], in which phenol reactions are considered, (3) the xylene model of Kukkadapu et al. [13], (4,5) the anisole models of Büttgen et al. [14] and Wagnon et al. [22], and (6) the guaiacol model of Nowakowska et al. [23].

Figures S3 to S5 show that simulations using the COLIBRI v2 model best reproduce the mole fraction of phenol, CO, ethylene, acetaldehyde, and acrolein, but, significant deviations are observed for compounds, such a cyclopentadiene or 1,3-butadiene. Latter products are better predicted by the models of Büttgen et al. [14] and Pratali Maffei et al. [15].

An initial flow rate analysis showed that the formation of cyclopentadiene is due to the reaction, $OH+C_6H_5OH=OH+CO+C_5H_6$, which was not considered neither by Büttgen et al. [14] and Pratali Maffei et al. [15], nor in Yuan's updated model for anisole [19]. This reaction, for which no sound justification was given by Yuan et al. [12], was therefore removed in COLIBRI v3.

Many theoretical studies have focused on the H-abstractions from phenol, its unimolecular decomposition, that of phenoxy radical, and other reactions involved in the first steps of phenol thermal decomposition. In oxidation, the start of phenol reactivity and products formation as well as the LBV are especially sensitive to the rate constants of the H--abstractions by OH and of the CO elimination from phenoxy radical yielding C_5H_5 radical and CO. The rate constants of these three reactions, found in literature in existing models [14–16,19] or theoretically calculated [15,24–27], are compared in Figure S6 where deviations of about a factor 10 are observed, whatever the reaction.

In COLIBRI v3, isomers of hydroxyphenyl, hydroxyphenoxy and catechol are differentiated. All kinetic calculations by Pratali Maffei et al. [15] are incorporated; they concern the reactions relevant to phenol pyrolysis, including the H-abstractions by H atoms. Other H-abstractions from phenol are updated with the data by Wang et al. [24].

Additionally, rate expressions related to hydroxyphenyl radicals were calculated at the G4 level of theory [28] as part of this study. They concern CO and water eliminations, isomerizations between phenoxy and hydroxyphenyl radical isomers as well as the oxygen addition to ortho-hydroxyphenyl leading to ortho-benzoquinone and the OH radical. Calculation details can be found in SM.

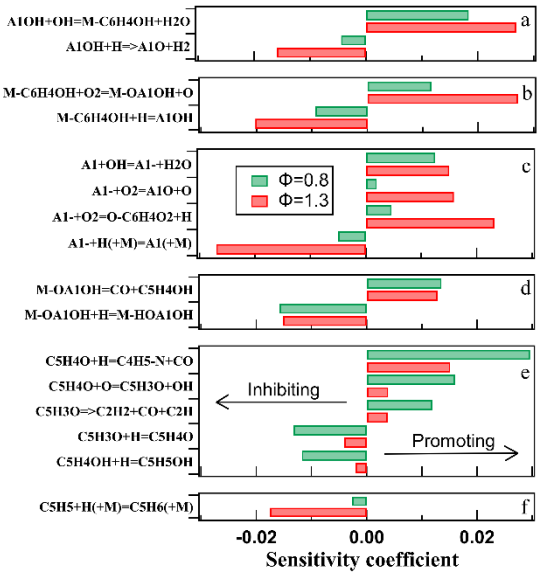

Fig.5. Sensitivity analysis for the most sensitive reactions involving C_{5+} reactions for the LBV at ϕ = 0.8 and 1.3. The reactions concern (a) phenol consumption, (b) hydroxyphenyl radicals, (c) benzene and phenyl radicals, (d) hydroxyphenoxy radicals, (e) the C_5H_XO submechanism, (f) cyclopentadienyl radicals. The species names are those used in the COLIBRI v3 model.

Quantum mechanical calculations were also used to qualitatively explore feasible pathways to experimentally detected C_{12}-C_{18} products in the low temperature range. While the initial dimerization products of phenoxy radicals are only modestly stable with respect to redissociation (see Table S3), the ortho-ortho dimer may rearrange through a low barrier transition state to the significantly more stable isomer 2,5'-biphenyldiol (see Figure S7), which is the only $C_{12}H_{10}O_2$ isomer identified experimentally (see Table S1) in the lower temperature range. H abstraction from 2,5'-biphenyldiol followed by intramolecular addition and release of OH would then lead to the observed dibenzofuran. Figure S8 shows that this sequence has only modest barriers. Similarly, if the intramolecular addition occurs to the aryl-C-H site followed by H-atom elimination, 3-hydroxydibenzofuran is formed, which is one of the proposed species for the $C_{12}H_8O_2$ product (see Figure S9). An extension of this chemistry naturally leads to a single $C_{18}H_{10}O_2$ isomer, in agreement with the experimental data (see Figure S10). Initial tests using approximated rate expressions for these reactions

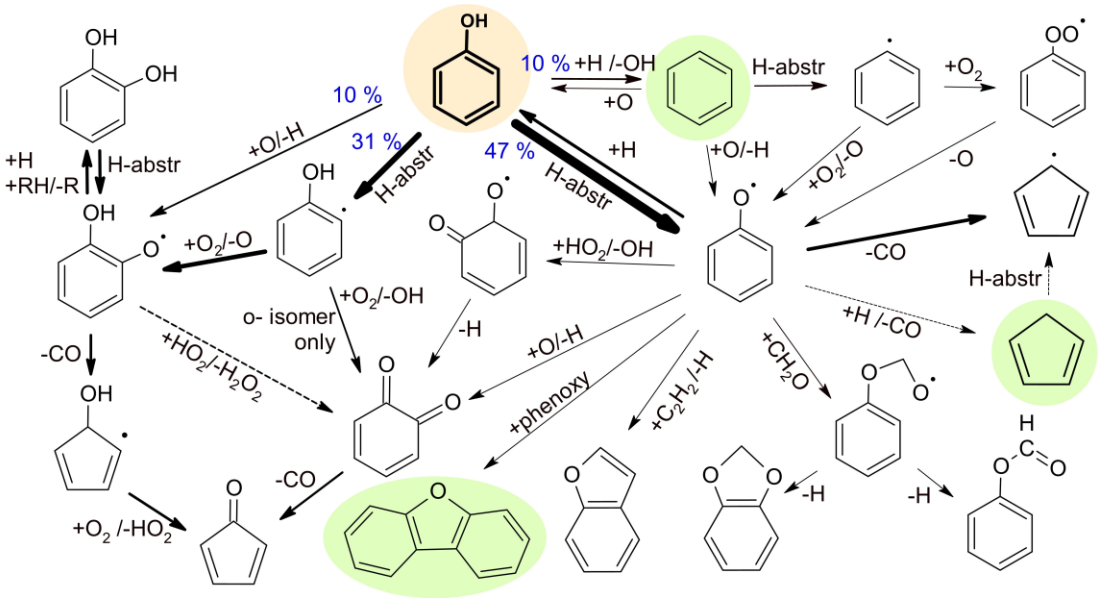

Fig.6. Flux analysis of phenol oxidation in JSR at 935 K corresponding to half of the fuel consumption. Only ortho-hydroxyphenyl, hydroxyphenoxy and catechol are drawn and represent the three ortho, meta and para isomers. The thickness of arrows is proportional to the flow.

showed an improvement of the predicted 2,5'-biphenyldiol yield, however its formation started at higher temperatures than seen experimentally. This indicates that more work is needed to address the low temperature reactivity seen in phenol oxidation. Table S4 lists all the updated reactions with rate constants given at 1 atm; the full pressure dependence can be found in the COLIBRI v3 mechanism file given in SM. Because of the sensitivity of results to the thermodynamic properties of the fuel and its first intermediates, the thermodynamic data of phenol, phenoxy and hydroxyphenyl are updated in this study, thanks to their calculation at the G4 level of theory. Validations against literature data are shown in SM.

3.2 Comparison between simulated and experimental results

As far as LBV are concerned, as it is shown in Figure 1, the updates in the COLIBRI v3 model significantly improve the predictions over a wide range of investigated equivalence ratios. Numerical values are close to the experimental ones and within the uncertainties, except for the lowest equivalence ratios for which the LBV is slightly underestimated.

Concerning JSR mole fractions, as it is shown in Figures 2 to 4, the agreement with COLIBRI v3 is similar to that with COLIBRI v2 for both reactants and main products such as CO, ethylene, acrolein, acetaldehyde, benzene, benzaldehyde and is significantly better for 1,3-butadiene and cyclopentadiene. Acetylene is a minor product, which is overestimated by one order of magnitude by COLIBRI model as well as by the other models of the literature (see Fig. S4). Despite being among major oxidation products, methane is overestimated by a factor of two by the COLIBRI model while numerical predictions of literature models are worse, as shown in Fig. S4. Obvious problems exist with the large underprediction of several C_{10+} species such as naphthalene and dibenzofuran. Some detected molecular weight growth species are not even included in the model.

3.3 Kinetic analyses

Kinetic analyses were performed both in flame and in JSR.

3.3.1. Flame kinetic analysis

The particularity of phenol in flame is that it is consumed through many different pathways as shown in Figure S12. H-abstractions leading to hydroxyphenyl radicals are the main decomposition pathways and highly promote the flame propagation. They are among the most sensitive reactions on the LBV as shown in the sensitivity analysis in Figure 5a. Reacting with O_2, hydroxyphenyl radical is involved in two pathways, one forming benzoquinone and OH, only for the ortho isomer, and the highly promoting branching reaction in competition with the inhibiting termination reaction with H-atoms in Figure 5b. The H-abstractions from the hydroxy group of phenol appear as an inhibiting pathway as it forms the resonantly stabilized phenoxy radical (see Figure 5a). Another important pathway is the ipso-addition of H-atoms to the hydroxy group forming benzene

because it mainly leads to phenyl, the key role of which is highlighted in Figure 5c notably because of its involvement both in the promoting branching reaction, phenyl+O_2→phenoxy+O, and in the inhibiting termination with H-atoms. The flux analysis in Figure S12 highlights one last consumption pathway of phenol: the ipso-addition of O-atoms to the aromatic ring. Because of its resonantly stabilized behavior, hydroxyphenoxy radical is at the heart of a strong competition between the inhibiting termination reaction with H-atoms forming catechol and the promoting CO elimination leading to hydroxycyclopentadienyl. Due to this competition, these reactions have a strong impact on LBV (see Figure 5d). In addition, in Figure 5e, the sensitivity analysis highlights a very sensitive submechanism composed of C_5H_XO species: cyclopentadienone (C_5H_4O), cyclopentadienol (C_5H_5OH) and its radicals (C_5H_4OH and C_5H_5O24). The only way to exit this loop submechanism is the decomposition of cyclopentadienone into smaller linear species or into C_5H_3O through H-abstractions. Therefore, these reactions, as well as the decomposition of C_5H_3O into smaller species, promote flame propagation. The terminations of C_5H_3O and C_5H_4OH with H-atoms respectively form back cyclopentadienone and produce cyclopentadienol in the inhibitory loop submechanism and strongly slow down the LBV. Interestingly, the CO elimination on hydroxyphenoxy radicals forming C_5H_4OH promotes the flame propagation even if it leads to the C_5 inhibiting submechanism. Cyclopentadiene and cyclopentadienyl radical are mainly produced from phenoxy and hydroxyphenyl radicals and constitutes another way to form C_{5-} species.

The most significant influence of the equivalence ratio in phenol flame is the inhibition of the C_5H_XO loop submechanism under rich condition coupled to a higher proportion of C_5H_4O and C_5H_3O decomposing into smaller linear species. Consequently, these reactions in figure 5e are not sensitive in rich mixture and most of other key reactions in figure 5 are even more sensitive.

3.3.2. JSR kinetic analysis

The flow analysis of the first pathways in phenol oxidation at 935 K is presented in Figure 6. The main decomposition pathways of phenol are the H-abstractions leading to phenoxy radicals; phenol+HO_2→phenoxy+H_2O_2 consumes 29% of the fuel and is the most sensitive reaction for the phenol mole fraction as shows Figure S13a. Phenoxy radicals mainly lead to cyclopentadienyl by CO elimination and re-form phenol by termination with H-atoms. Phenoxy radicals are also involved in additions and terminations typical of this temperature range [2,16] leading to benzodioxole, benzofuran and dibenzofuran, which were detected experimentally. Phenoxy radicals are also formed through minor pathways coming from the formation of benzene by ipso-addition with H-atoms on the hydroxy group of phenol. The second main way to decompose phenol are the H-abstractions on the aromatic ring. The hydroxyphenyl radicals mainly react with O_2 through branching reactions leading to hydroxyphenoxy radicals, also directly formed from phenol. The Figure S13b-c highlights that phenoxy-like radicals are at the heart of a competition between inhibiting termination reactions with H-atoms and HO_2, and alternative promoting pathways, notably CO eliminations. Other sensitive reactions concern the fuel consumption and H_2O_2→2OH multiplying OH radicals. Finally, the flow analysis contains numerous cyclopentadienone pathways (not experimentally detected, but leading to quantified C_2 products), with C_5H_4OH and ortho-benzoquinone as intermediates, as in flame.

4. Conclusion

This paper presents the first detailed kinetic model for phenol oxidation validated on new experimental data, both LBV measurements and products quantification in a JSR. After revising the phenol related rate constants using recent literature data and theoretical calculations, a global satisfactory agreement can be obtained between measured and simulated data. However, some species like acetylene, methane and $C_{12\leq}$ compounds are still poorly estimated, what calls for future works on phenol kinetic in order to perfectly understand its combustion behaviour. Finally, the key role of phenoxy-like and phenyl radicals, as well as of the C_5H_XO submechanism, is highlighted in kinetic analyses in both JSR and flame.

Declaration of competing interest

The authors declare that they have no known competing financial interests or personal relationships that could have appeared to influence the work reported in this paper.

Acknowledgements

We acknowledge funding from the European Union's Horizon 2020 research and innovation program (BUILDING A LOW-CARBON, CLIMATE RESILIENT FUTURE: SECURE, CLEAN AND EFFICIENT ENERGY) under Grant Agreement No 101006744 and of COST (European Cooperation in Science and Technology) Action CYPHER CA22151. The content presented in this document represents the views of the authors, and the European Commission has no liability in respect of the content. HHC acknowledges support by the Aragon Government (T22_20R).

Supplementary material

Supplementary material associated with this article can be found, in the online version, at doi: xxx.

5. References

[1] M.U. Alzueta, P. Glarborg, K. Dam-Johansen, Experimental and kinetic modeling study of the oxidation of benzene, International Journal of Chemical Kinetics 32 (2000) 498–522.

[2] I. Meziane, N. Delort, O. Herbinet, R. Bounaceur, F. Battin-Leclerc, A comparative study of the oxidation of toluene and the three isomers of xylene, Combustion and Flame 257 (2023) 113046.

[3] R. Azargohar, K.L. Jacobson, E.E. Powell, A.K. Dalai, Evaluation of properties of fast pyrolysis products obtained, from Canadian waste biomass, Journal of Analytical and Applied Pyrolysis 104 (2013) 330–340.

[4] M. Pelucchi, C. Cavallotti, A. Cuoci, T. Faravelli, A. Frassoldati, E. Ranzi, Detailed kinetics of substituted phenolic species in pyrolysis bio-oils, Reaction Chemistry & Engineering 4 (2019) 490–506.

[5] F. Battin-Leclerc, N. Delort, I. Meziane, O. Herbinet, Y. Sang, Y. Li, Possible use as biofuels of monoaromatic oxygenates produced by lignin catalytic conversion: A review, Catalysis Today 408 (2023) 150–167.

[6] Y.Z. He, W.G. Mallard, W. Tsang, Kinetics of hydrogen and hydroxyl radical attack on phenol at high temperatures, Journal of Physical Chemistry 92 (1988) 2196–2201.

[7] C. Horn, K. Roy, P. Frank, T. Just, Shock-tube study on the high-temperature pyrolysis of phenol, Symposium (International) on Combustion 27 (1998) 321–328.

[8] A.B. Lovell, K. Brezinsky, I. Glassman, The gas phase pyrolysis of phenol, International Journal of Chemical Kinetics 21 (1989) 547–560.

[9] K. Brezinsky, M. Pecullan, I. Glassman, Pyrolysis and Oxidation of Phenol, J. Phys. Chem. A 102 (1998) 8614–8619.

[10] J.A. Manion, R. Louw, Rates, products, and mechanisms in the gas-phase hydrogenolysis of phenol between 922 and 1175 K, J. Phys. Chem. 93 (1989) 3563–3574.

[11] R. Bounaceur, I. Da Costa, R. Fournet, F. Billaud, F. Battin-Leclerc, Experimental and modeling study of the oxidation of toluene, International Journal of Chemical Kinetics 37 (2005) 25–49.

[12] W. Yuan, Y. Li, P. Dagaut, J. Yang, F. Qi, Investigation on the pyrolysis and oxidation of toluene over a wide range conditions. I. Flow reactor pyrolysis and jet stirred reactor oxidation, Combustion and Flame 162 (2015) 3–21.

[13] G. Kukkadapu, D. Kang, S.W. Wagnon, K. Zhang, M. Mehl, M. Monge-Palacios, H. Wang, S.S. Goldsborough, C.K. Westbrook, W.J. Pitz, Kinetic modeling study of surrogate components for gasoline, jet and diesel fuels: C7-C11 methylated aromatics, Proceedings of the Combustion Institute 37 (2019) 521–529.

[14] R.D. Büttgen, M. Tian, Y. Fenard, H. Minwegen, M.D. Boot, K.A. Heufer, An experimental, theoretical and kinetic modelling study on the reactivity of a lignin model compound anisole under engine-relevant conditions, Fuel 269 (2020) 117190.

[15] L. Pratali Maffei, M. Pelucchi, T. Faravelli, C. Cavallotti, Theoretical study of sensitive reactions in phenol decomposition, React. Chem. Eng. 5 (2020) 452–472.

[16] N. Delort, M. Ismahane, M. Framinet, R. Bounaceur, J. Bourgalais, F. Battin-Leclerc, O. Herbinet, An experimental and modelling investigation of the combustion of anisole and guaiacol, Fuel 362 (2024) 130832.

[17] K.J. Bosschaart, L.P.H. de Goey, The laminar burning velocity of flames propagating in mixtures of hydrocarbons and air measured with the heat flux method, Combust. Flame 136 (2004) 261–269.

[18] P. Dirrenberger, P.A. Glaude, R. Bounaceur, H. Le Gall, A.P. da Cruz, A.A. Konnov, F. Battin-Leclerc, Laminar burning velocity of gasolines with addition of ethanol, Fuel 115 (2014) 162–169.

[19] W. Yuan, T. Li, Y. Li, M. Zeng, Y. Zhang, J. Zou, C. Cao, W. Li, J. Yang, F. Qi, Experimental and kinetic modeling investigation on anisole pyrolysis: Implications on phenoxy and cyclopentadienyl chemistry, Combustion and Flame 201 (2019) 187–199.

[20] R.J. Kee, F.M. Rupley, J.A. Miller, M.E. Coltrin, J.F. Grcar, E. Meeks, H.K. Moffat, A.E. Lutz, G. Dixon-Lewis, M.D. Smooke, CHEMKIN collection, release 3.6, reaction design, Inc., San Diego, CA 20 (2000).

[21] U. Burke, W.K. Metcalfe, S.M. Burke, K.A. Heufer, P. Dagaut, H.J. Curran, A detailed chemical kinetic modeling, ignition delay time and jet-stirred reactor study of methanol oxidation, Combustion and Flame 165 (2016) 125–136.

[22] S.W. Wagnon, S. Thion, E.J.K. Nilsson, M. Mehl, Z. Serinyel, K. Zhang, P. Dagaut, A.A. Konnov, G. Dayma, W.J. Pitz, Experimental and modeling studies of a biofuel surrogate compound: laminar burning velocities and jet-stirred reactor measurements of anisole, Combustion and Flame 189 (2018) 325–336.

[23] M. Nowakowska, O. Herbinet, A. Dufour, P.A. Glaude, Kinetic Study of the Pyrolysis and Oxidation of Guaiacol, J. Phys. Chem. A 122 (2018) 7894–7909.

[24] Q.-D. Wang, M.-M. Sun, J. Liang, Theoretical study of the hydrogen abstraction reactions from substituted phenolic species, Computational and Theoretical Chemistry 1196 (2021) 113120.

[25] F. Xu, H. Wang, Q. Zhang, R. Zhang, X. Qu, W. Wang, Kinetic Properties for the Complete Series Reactions of Chlorophenols with OH Radicals—Relevance for Dioxin Formation, Environ. Sci. Technol. 44 (2010) 1399–1404.

[26] B. Shu, J. Herzler, S. Peukert, M. Fikri, C. Schulz, A Shock Tube and Modeling Study about Anisole Pyrolysis Using Time-Resolved CO Absorption Measurements, International Journal of Chemical Kinetics 49 (2017) 656–667.

[27] H.-H. Carstensen, A.M. Dean, A quantitative kinetic analysis of CO elimination from phenoxy radicals, International Journal of Chemical Kinetics 44 (2012) 75–89.

[28] L.A. Curtiss, P.C. Redfern, K. Raghavachari, Gaussian-4 theory, The Journal of Chemical Physics 126 (2007) 084108.